Size Effects of Graphene Oxide on Mixed Matrix Membranes for CO_2 Separation

Jie Shen, Mengchen Zhang, Gongping Liu, Kecheng Guan, and Wanqin Jin
State Key Laboratory of Materials-Oriented Chemical Engineering, Jiangsu National Synergetic Innovation Center for Advanced Materials, Nanjing Tech University, 5 Xinmofan Road, Nanjing 210009, P. R. China

DOI 10.1002/aic.15260
Published online in Wiley Online Library (wileyonlinelibrary.com)

Graphene oxide (GO)-polyether block amide (PEBA) mixed matrix membranes were fabricated and the effects of GO lateral size on membranes morphologies, microstructures, physicochemical properties, and gas separation performances were systematically investigated. By varying the GO lateral sizes (100–200 nm, 1–2 μm, and 5–10 μm), the polymer chains mobility, as well as the length of the gas channels could be effectively manipulated. Among the as-prepared membranes, a GO-PEBA mixed matrix membrane (GO-M-PEBA) containing 0.1 wt % medium-lateral sized (1–2 μm) GO sheets showed the highest CO_2 permeation performance (CO_2 permeability of 110 Barrer and CO_2/N_2 mixed gas selectivity of 80), which transcends the Robeson upper bound. Also, this GO-PEBA mixed matrix membrane exhibited high stability during long-term operation testing. Optimized by GO lateral size, the developed GO-PEBA mixed matrix membrane shows promising potential for industrial implementation of efficient CO_2 capture. © 2016 American Institute of Chemical Engineers *AIChE J*, 00: 000–000, 2016
Keywords: graphene oxide, gas channel, size effect, mixed matrix membrane, CO2 separation

Introduction

Efficient and environmentally friendly purification technologies are important research topics for dealing with many global challenges such as water treatment, natural gas purification, and CO_2 capture. Membrane-based separation, aimed at decreasing energy consumption, production costs and equipment size, is considered to be a promising method compared to distillation and adsorption.[1–3] However, traditional polymeric membranes suffer from trade-off properties,[4–6] resulting in great difficulty in simultaneously obtaining high selectivity and permeability. Recently, the groundbreaking contribution of Geim and coworkers on the two-dimensional (2D) material graphene[7–9] and its derivatives, such as graphene oxide (GO), offers great potential for the development of a brand new generation of ultra-high performance and energy-efficient membranes, owing to their unique atomic-thick structures with outstanding mechanical strength, chemical stability, low transport resistance, and narrow distribution of pore size.[10] To date, there are mainly three types of graphene-based membranes, namely porous graphene membranes, graphene laminate membranes, and graphene-composite membranes.[10,11] Porous graphene membranes are predicted to be highly selective because of the elaborate physical perforation on the graphene layer.[12] However, these are high-cost and it is a great challenge to uniformly drill the pores in large area. Graphene laminate membranes can be easily fabricated by dip-coating,[13] filtration,[14,15] and spin-coating[16] methods, which have been widely studied by researchers. However, they still face the difficulty of the inevitable generation of non-selective defects, which are unfavorable for efficient separation.[17] Moreover, brittle graphene laminate membranes without reliable modules are difficult to use in practical applications.[10] Fortunately, graphene-composite membranes combine the advantages of both graphene and other materials (such as polymer), exhibiting enhanced separation performance and fabrication feasibility, which are more practical for industrial applications.[18,19]

So far, many organic and inorganic materials have been embedded into the polymer matrix to obtain mixed matrix membranes (MMMs), in an attempt to achieve higher permeability and selectivity. The dispersed filler materials include carbon molecular sieves,[5,20,21] silica,[22–24] zeolite[5,25–27] mesoporous materials,[28] carbon nanotube,[29] and metal organic frameworks.[30,31] As oxidized graphene, GO is now considered to be a novel material for developing MMMs. Compared with pristine graphene, GO possesses more oxygen-containing groups which provide versatile sites for interacting with polymeric chains. Owing to its hydrophilic characteristic, GO was first added into the polymeric membranes for water treatment. Ismail et al.[32] developed a GO-polysulfone membrane with improved hydrophilicity, water flux, and salt rejection. The antifouling property can also be enhanced by incorporating GO sheets into polyethersulfone ultrafiltration membranes.[33] In addition, the polar groups of –COOH and –OH on GO sheets can generate specific interactions with CO_2 molecules, which are beneficial for the solubility selectivity of CO_2/gas separation.[16,34] In our previous work, we discovered that GO can be effectively engineered in polymeric environment by

Additional Supporting Information may be found in the online version of this article.

Correspondence concerning this article should be addressed to W. Jin at wqjin@njtech.edu.cn.

forming hydrogen bonding frameworks between GO and polymer. The assembled GO laminates provided molecular sieving gas channels for fast and selective CO_2 separation.[35] However, many factors that can greatly influence the membrane structure and separation performances have not been well studied. Indeed, by tuning the chemical properties,[36] preparation methods[37] and pH values of the GO suspension,[38] GO-based MMMs can exhibit different molecular transport behaviors. One of the most important factors is the GO lateral size, which is worth of study in detail. On the one hand, varying lateral size can change the diffusion length of the permeate molecules, as demonstrated in other reports.[16,39] On the other hand, the polymer chains packing behaviors can be affected by varying the lateral size. This is due to the fact that polymer chains are excluded when large sized fillers are incorporated into the polymer matrix.[24,40,41] Therefore, the free volume of the polymeric material is likely to be changed, which will also affect the molecular transport in the membrane. Thus, a systematic study of the effects of GO lateral size on MMMs is needed to further understand the membrane microstructures and gas transport properties.

In this work, GO nanosheets with different lateral sizes were engineered to fabricate GO-polyether block amide (PEBA) MMMs. The size effects of GO on the membranes morphologies, microstructures, and physicochemical properties were systematically investigated. The CO_2/N_2 separation behaviors of the as-prepared GO-PEBA MMMs with distinct lateral sizes were also studied to further understand the gas transport mechanism in the GO-based gas channels.

Experimental

Materials

GO powders (provided from Nanjing JCNANO Tech Co., China) were prepared by the modified Hummers' method.[42] Typically, 10 g of graphite powder and 5 g of $NaNO_3$ were added into 230 mL of 98 wt % H_2SO_4 under stirring for 1 h. Then, 30 g of $KMnO_4$ was slowly put into the mixture solution, while maintaining the temperature below 20°C for about 2 h. Subsequently, the reaction temperature was carefully increased to 35°C and stirred for 0.5 h. Then, 460 mL deionized water was slowly added to the system. After that, the mixture was heated to 98°C and stirred for 15 min. The reaction was stopped by adding 1.4 L of deionized water, followed by the addition of 100 mL of H_2O_2 until the mixture turned yellow. The mixture was washed with 2 L 1 mol/L of HCl and a large amount of deionized water. The resulting solid was dried and dissolved in deionized water followed by sonication under 35 kHz for 0.5 h. The stable GO dispersion was finally obtained after centrifugation at 2000 rpm for 30 min. GO sheets with different sizes were obtained *via* different centrifugation and sonication treatments. First, the GO dispersion was centrifuged at 4000 rpm for 1 h. The sediment was collected as the maximum size GO, this was denoted as GO-L. Meanwhile, the supernatant was then treated under distinct sonication conditions to acquire medium sized GO (100 W sonication) denoted as GO-M and minimum sized GO (400 W sonication) denoted as GO-S. PEBAX MH 1657 was provided from Arkema, France. Ethanol was supplied by the Wuxi City Yasheng Chemical Co. N_2 and CO_2 with the purities of 99.999% were purchased from the Nanjing Special Gases Co. Polyvinylidene fluoride (PVDF) supports with average pore size of 450 nm were obtained from Solvay, USA. Deionized water was used in all the experiments.

Membrane preparation

The GO-PEBA MMMs were fabricated by a solution casting method. GO powders with different lateral sizes and oxidation degrees were dispersed in a solvent mixture of 70 wt % ethanol and 30 wt % water and then treated by ultrasonication for 1 h. After that, PEBA pellets were added into the solvent with stirring under 80°C for 12 h. After eliminating the bubbles, the mixed solution was cast on PVDF substrates to fabricate flat composite membranes. The corresponding free-standing membranes were fabricated by casting the mixed solution onto the glass. The membranes were finally formed by evaporating the solvent at room temperature for 2 days and, then drying in a vacuum oven at 70°C for 48 h. The pristine PEBA membrane could be fabricated according to a similar procedure without the filling of GO.

Characterization

The dispersion and the sizes of GO sheets and the surface morphologies of the as-prepared membranes were obtained by atomic force microscopy (AFM, XE-100, Park SYSTEMS, Korea) operated in non-contact mode. Fourier transform infrared (FTIR, AVATAR-FT-IR-360, Thermo Nicolet, USA) spectra was used to characterized the functionalized groups on GO. X-ray photoelectron spectroscopy (XPS, Thermo ESCALAB 250, USA) was conducted and recorded using monochromatized Al Ka radiation (1486.6 eV). The crystalline structure of the GO powders and GO-PEBA MMMs were analyzed by X-ray diffraction (XRD, Bruker, D8 Advance) using Cu Kα radiation ($\lambda = 1.54$ Å) at 40 kV and 15 mA at room temperature. Raman spectroscopy (LabRAM HR, HORIBA, France) was carried out with 514 nm wavelength incident laser light with the range of 500–4000 cm^{-1} to distinguish the ordered and disordered carbon structures. Field emission scanning electron microscope (FESEM, S4800, Hitachi, Japan) was used to observe the morphologies of the GO-PEBA MMMs. To further characterize the glass transition temperatures (Tg) of the GO-PEBA MMMs, the differential scanning calorimetry (DSC, Q2000, TA Instruments, USA) measurements were carried out from -80 to 40°C in N_2 atmosphere. The thermal properties of GO and the GO-PEBA MMMs were characterized by thermogravimetric analysis (TGA, NETZSCH STA 449F3) from room temperature to 800°C with the rate of 10°C min^{-1}.

Gas permeation measurements

Both pure gas and mixed gas permeation were carried out to study the CO_2/N_2 separation behaviors of the as-prepared GO-PEBA MMMs using constant-pressure, variable-volume method, which was reported in our previous work.[43] The schematic of apparatus is shown in Supporting Information Figure 1. The gas flow rates were detected with a bubble flow meter. The permeation measurements of each gas were performed more than five times. The pure gas permeation tests of CO_2 and N_2 were conducted under a pressure of 0.3 MPa at 25°C. The gas permeability was calculated after the system reached steady-state using the following equation:

$$P = \frac{QL}{\Delta PA} \tag{1}$$

where P is the gas permeability [1 Barrer $= 10^{-10}$ cm^3

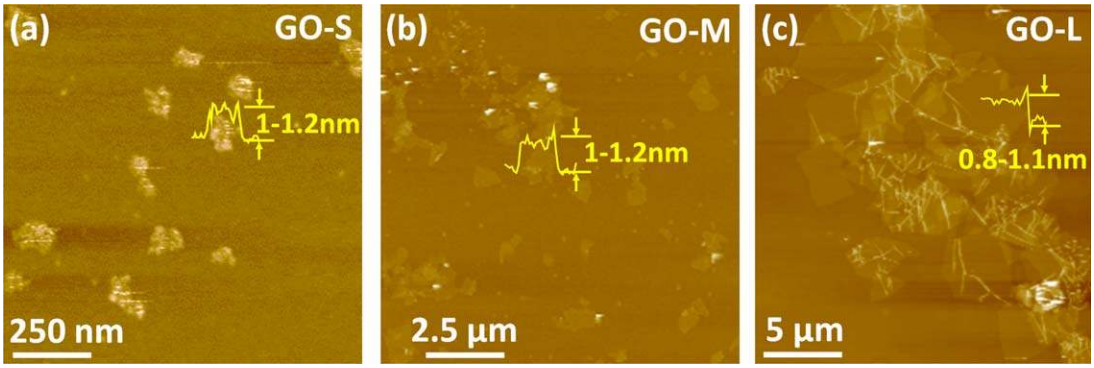

Figure 1. AFM images for GO sheets with different lateral sizes.

(a–c) Revealed that the lateral sizes are 100–200 nm, 1–2 μm, and 5–10 μm, respectively. [Color figure can be viewed in the online issue, which is available at wileyonlinelibrary.com.]

(standard temperature and pressure—STP) cm/(cm^2 · s · cmHg)], Q is the permeate rate of gas (cm^3/s) at STP, L is the membrane thickness (cm), ΔP is the transmembrane pressure (cmHg), and A is the membrane effective area (cm^2). The ideal selectivity of CO_2/N_2 can be calculated by the ratio of the permeability of the individual gas which can be expressed as follows:

$$\alpha = \frac{P_A}{P_B} \tag{2}$$

The mixed gas permeation tests were also performed at 25°C and atmosphere pressure. A binary mixture of 50% CO_2 and 50% N_2 (vol %) was used as the feed while CH_4 was selected as the sweep gas. The selectivity for binary gas mixtures can be calculated by the following equation:

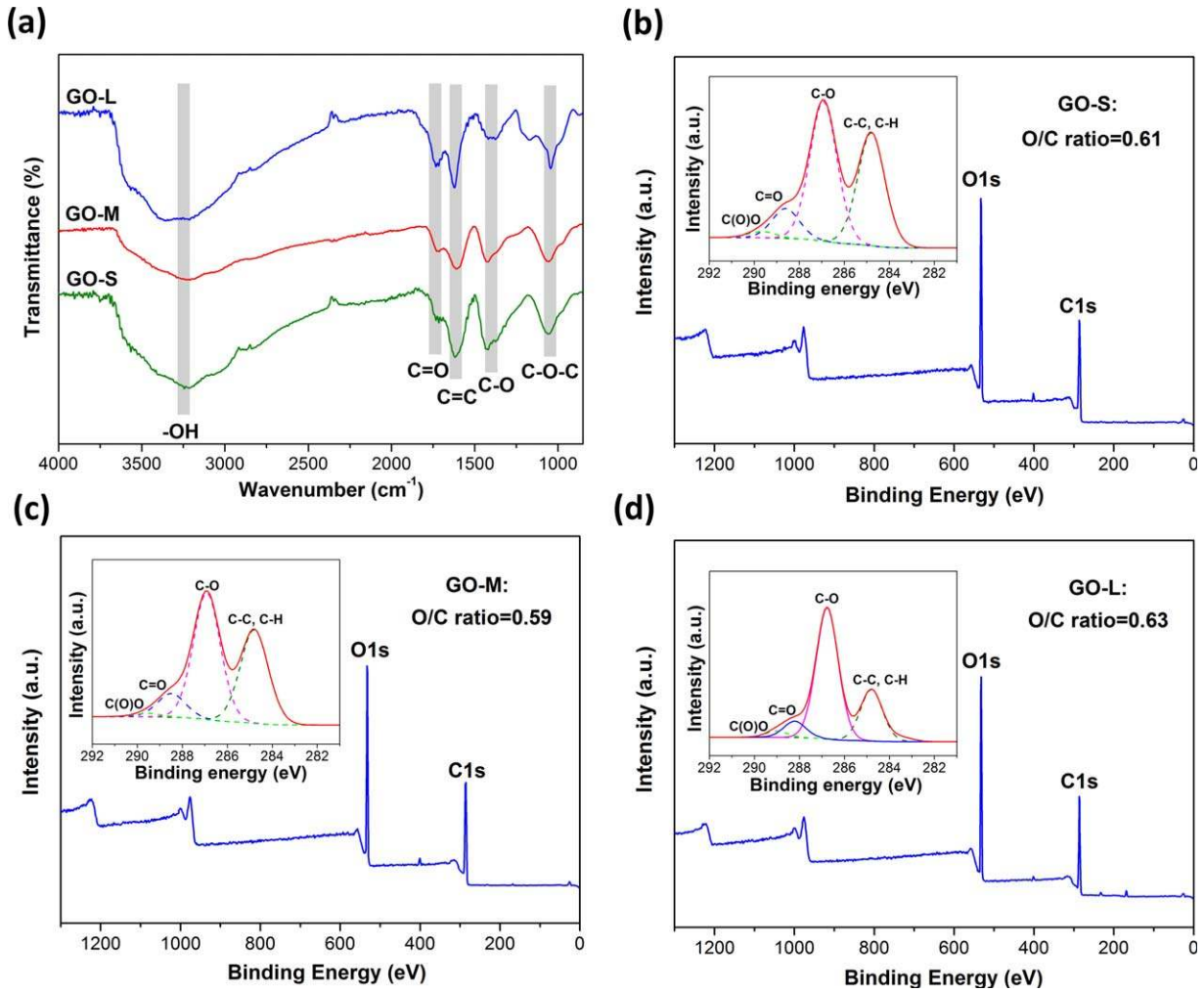

Figure 2. (a) FTIR spectra of GO with different lateral sizes, (b–d) are the wide scan of XPS inserted with patterns of narrow scan.

[Color figure can be viewed in the online issue, which is available at wileyonlinelibrary.com.]

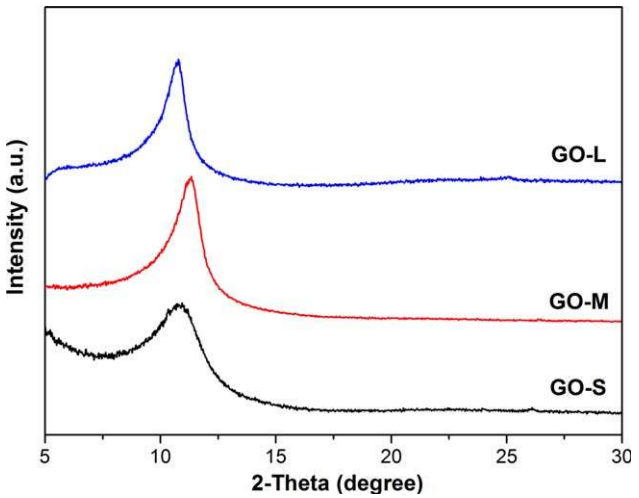

Figure 3. XRD patterns for GO with different lateral sizes.

[Color figure can be viewed in the online issue, which is available at wileyonlinelibrary.com.]

$$\alpha_{A/B} = \frac{y_A/y_B}{x_A/x_B} \tag{3}$$

where x and y are the volumetric fractions of the one component in the feed and permeate, respectively. When the membranes were tested in a humid state, the feed and sweep gases were both humidified by water bottles. After humidifying, the relative humidity can be increased from 20 to 85%.

Results and Discussion

GO characterization

The morphologies of GO sheets with different lateral sizes were clearly characterized by AFM and the results are shown in Figure 1. It can be found that all the GO sheets were exfoliated to single layer and dispersed homogenously in the ethanol/water mixed solvent. The GO sheets showed a typical wrinkled morphology, which has been reported elsewhere.[44] The thickness of the GO sheets was about 1 nm and the lateral sizes were from 100–200 nm, 1–2 μm, and 5–10 μm. Therefore, the GO-PEBA

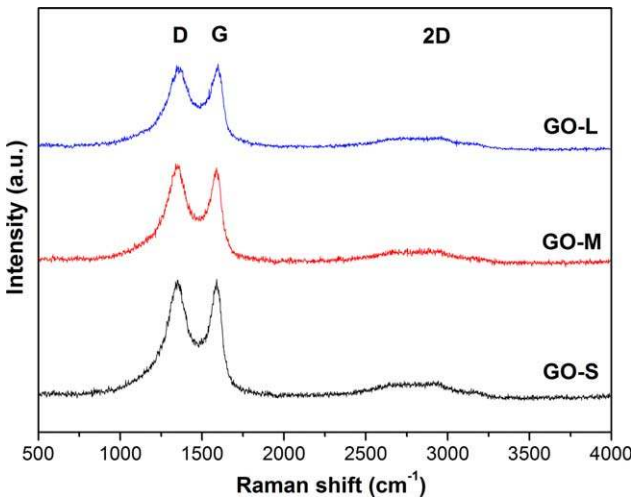

Figure 4. Raman spectra for GO with different lateral sizes.

[Color figure can be viewed in the online issue, which is available at wileyonlinelibrary.com.]

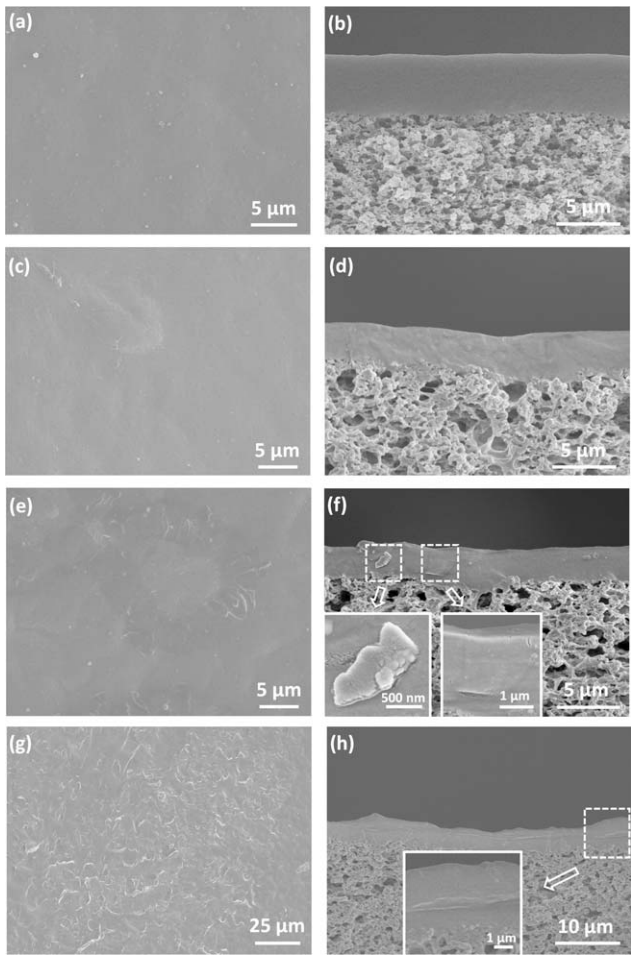

Figure 5. Surface FESEM images of (a), (c), (e), and (g) and cross-section FESEM images of (b), (d), (f), and (h) for bare PEBA, GO-S-PEBA, GO-M-PEBA, and GO-L-PEBA membranes, respectively.

All these membranes are with GO content of 0.1 wt %.

MMMs with different sized GO sheets are expected to exhibit distinct gas permeation behaviors, as discussed later.

FTIR was conducted to analyze the functional groups of the different sized GO sheets, as shown in Figure 2a. The characteristic peaks of 3270 and 1290 cm^{-1} represent –OH and C–O, respectively. The stretching vibration at 1060 cm^{-1} indicates the functionalized group of C–O–C. The absorption bands at 1585 and 1730 cm^{-1} are from C=C and C=O, respectively. All these results show the typical chemical structure of GO, which agrees well with the Lerf–Klinowski Model.[45] The XPS results in Figures 2b–d showed the different functional groups of GO, namely C–C, C–H (~284.8 eV), C–O (~286.7 eV), C=O (~288.4 eV), and C(O)O (~289.6 eV). In addition, it can be found that all the GO sheets with distinct lateral sizes have high O/C ratios of about 0.6, which is beneficial for interacting with the polymer chains, as well as for providing CO_2-selective gas channels. Moreover, the embedding of a large amount of functional groups obviously enlarged the interlayer spacing between the graphene sheets, thus providing more space for molecular transport.

The crystal structure of GO was characterized by XRD, as shown in Figure 3. It can be seen that after the oxidation process, the interlayer spacing between graphene layers increased because of the introduction of oxygen-containing groups. The

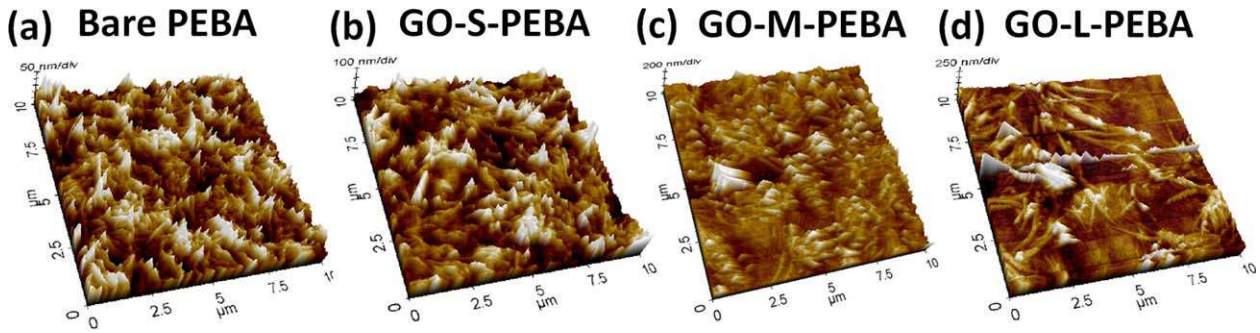

Figure 6. AFM images of the surfaces of bare PEBA membrane and GO-PEBA MMMs, scan area: 10 μm × 10 μm.

[Color figure can be viewed in the online issue, which is available at wileyonlinelibrary.com.]

characteristic peaks for all the samples are at about $2\theta = 11°$, which indicates a d-spacing of 0.8 nm. It has been proven that the interlayer spacing of GO laminates can exhibit a molecular sieving effect after being tailored by assembling in polymeric environment.[35] Thus, for small molecules, such as CO_2, fast transport through the GO interlayer gallery is possible, while larger molecules cannot enter into these channels.

Raman spectroscopy is applied to further analyze the microstructure of GO (Figure 4). Generally, Raman spectroscopy is highly sensitive in distinguishing ordered and disordered carbon structures, exhibiting characteristic peaks of D, G, and 2D bonds. The D bond indicates local defects/disorders, the G bond is assigned to the graphitized structure while the 2D bond is used to monitor the number of layers.[46,47] Thereby, a smaller I_D/I_G intensity ratio tends to a lower amount of defects/disorders in the GO plane. The I_D/I_G ratios of GO with different lateral sizes are all around 1.0, which is consistent with the literature,[34] demonstrating the well-organized graphene laminar with a low defective microstructure.

Membrane characterization

The single-layered GO sheets were dispersed in polymeric membranes to be assembled into laminate structure. The morphologies of the bare PEBA membrane and GO-PEBA MMMs were observed using FESEM, which are shown in Figure 5. For comparison, the surface and cross-section images of the bare PEBA membrane and GO-PEBA MMMs were presented. GO-PEBA MMMs using GO sheets with different lateral sizes of 100–200 nm, 1–2 μm, and 5–10 μm were denoted as GO-S-PEBA, GO-M-PEBA, and GO-L-PEBA, respectively. After the casting process, both the bare PEBA membrane and GO-PEBA MMMs active layers were uniformly coated on the PVDF supports and adhered well to the support layers. The surfaces of the prepared bare PEBA membrane and GO-PEBA MMMs were dense and defect-free. The membranes with the composite structures could be observed clearly from the FESEM images. For the bare PEBA membrane, the active layer is highly smooth as shown in Figures 5a, b. However, when added with GO sheets, rough morphologies appeared in the active layers. More and more bulges were generated with the increase in GO sheets lateral sizes. These indicate that the lateral sizes of GO sheets significantly affected the membranes morphologies and GO sheets were not completely in the horizontal direction in the polymeric membrane. In contrast, they were in random orientations, so that various bulges can be formed in the GO-PEBA MMMs surfaces and cross-sections. Moreover, the GO laminates assembled in the GO-M-PEBA membrane were clearly observed and are shown in Figure 5f. It shows the typical laminar structure of well-defined GO stacks, arranged in the vertical and inclined directions. The lateral sizes of these GO sheets were in the range of 1–2 μm, consistent with the AFM characterization of the GO nanosheets in Figure 1. GO laminates in the vertical and slightly inclined directions are beneficial for providing numerous fast and selective gas channels for high efficiency CO_2 permeation. However, it can be observed that GO sheets with lateral size of 5–10 μm (even larger than the membrane thickness) were more inclined to arrange in the horizontal direction (Figure 5h), which is considered to hinder gas transport.

The surface morphologies of GO-PEBA MMMs were further studied by AFM characterization. As shown in Figure 6, the surface of bare PEBA was covered with a significant amount of small bulges which is due to the special chemical composition of the PEBA polymer. PEBA is a type of segmented copolymer that contains a soft rubbery PE phase and a hard glassy PA phase, which can lead to microphase separation.[48] However, some large flake-like bulges appeared after the GO sheets were embedded into the polymer chains. Therefore, as proven by the FESEM images, the surface roughness increased gradually with the GO sheets lateral sizes. However, it should be noted that the GO-L-PEBA membrane exhibited the largest surface roughness (Table 1, also seen in the FESEM image of Figures 5g, h). It is considered to be dominated by the size effect of the GO sheets. GO sheets are well demonstrated to have wrinkled surfaces,[49] which can significantly influence the membrane morphology, especially for GO with a large lateral size. Also, the packing behaviors of polymer chains can be obviously influenced by large sized GO sheets. Generally, polymer chains could be excluded when large sized fillers were incorporated into the polymer matrix, as demonstrated in the literature.[24,40,41]

The microstructures of the GO-PEBA MMMs with different GO sheet lateral sizes were then investigated by XRD (Figure 7a). It could be seen that the crystallization properties changed as a result of GO sheet lateral size. PEBA is a semicrystalline copolymer which consists of both a crystalline phase of PA6 and an amorphous phase of PEO. The sharp X-ray diffraction peak represents the crystalline region of PA6 while the amorphous PEO exhibits a broad peak.[50] The characteristic peaks ranged from 15° to 25°, in agreement with earlier work.[51,52] The intensity of the characteristic peak of PA6 gradually increased as the GO sheets lateral sizes became larger. This is probably

Table 1. Surface Roughness Parameters of Membranes

Membrane	Bare PEBA	GO-S-PEBA	GO-M-PEBA	GO-L-PEBA
Ra (nm)	28.793	37.012	48.253	73.021
Rq (nm)	22.426	28.633	36.224	47.586

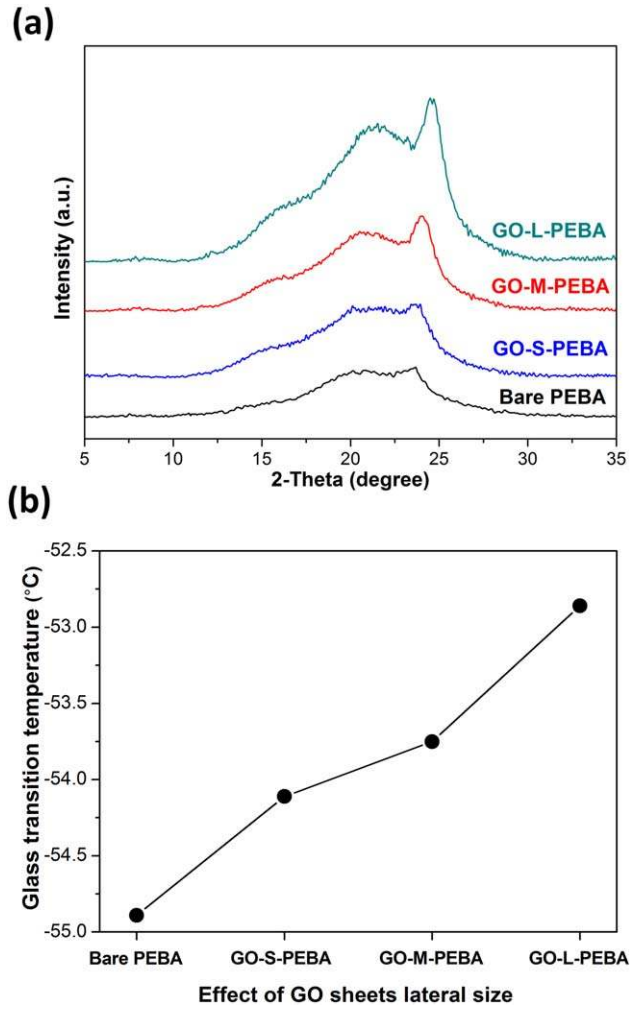

Figure 7. (a) XRD spectra of bare PEBA membrane and GO-PEBA MMMs with different GO lateral sizes. (b) Effect of GO lateral sizes on the glass transition temperatures of PEBA.

[Color figure can be viewed in the online issue, which is available at wileyonlinelibrary.com.]

because of the large amount of hydrogen frameworks formed between GO and the PEBA molecules, which efficiently restricted the mobility of the PEBA chains. GO sheets with larger sizes could increase the interaction area to further enhance the restriction effect. This was further demonstrated by the results of TGA, as shown in Supporting Information Figure 2. DSC measurements (Figure 7b) showed that Tg increased gradually with GO lateral size, which suggests the trend of the glass transition of polymer. This leads to rigid stacking of the polymer chains, so that the free volume can be lowered.

Effect of GO lateral size on CO_2/N_2 separation performance

GO sheets can be assembled to well-defined laminar structure with fast and selective gas transport channels in polymeric environment.[35] In fact, both the content of GO and GO sheet lateral size are of great significance in the controllable engineering of these gas channels, which is important in manipulating the membranes microstructures and the gas transport behaviors. For example, GO content controls the amount and uniform dispersion of the transport channels. Gas permeation through the GO-S-PEBA, GO-M-PEBA, and GO-L-PEBA membranes with different GO contents was systematically carried out and is shown in Figure 8. For the GO-S-PEBA and GO-M-PEBA membranes, the amount of gas channels increased with the GO contents, so the separation performance were in the trend of increasing at relatively low GO content. Moreover, the GO content influences the dispersion character of the gas channels in the polymeric environment. The "critical points" of the gas permeability appeared at 0.2 wt %

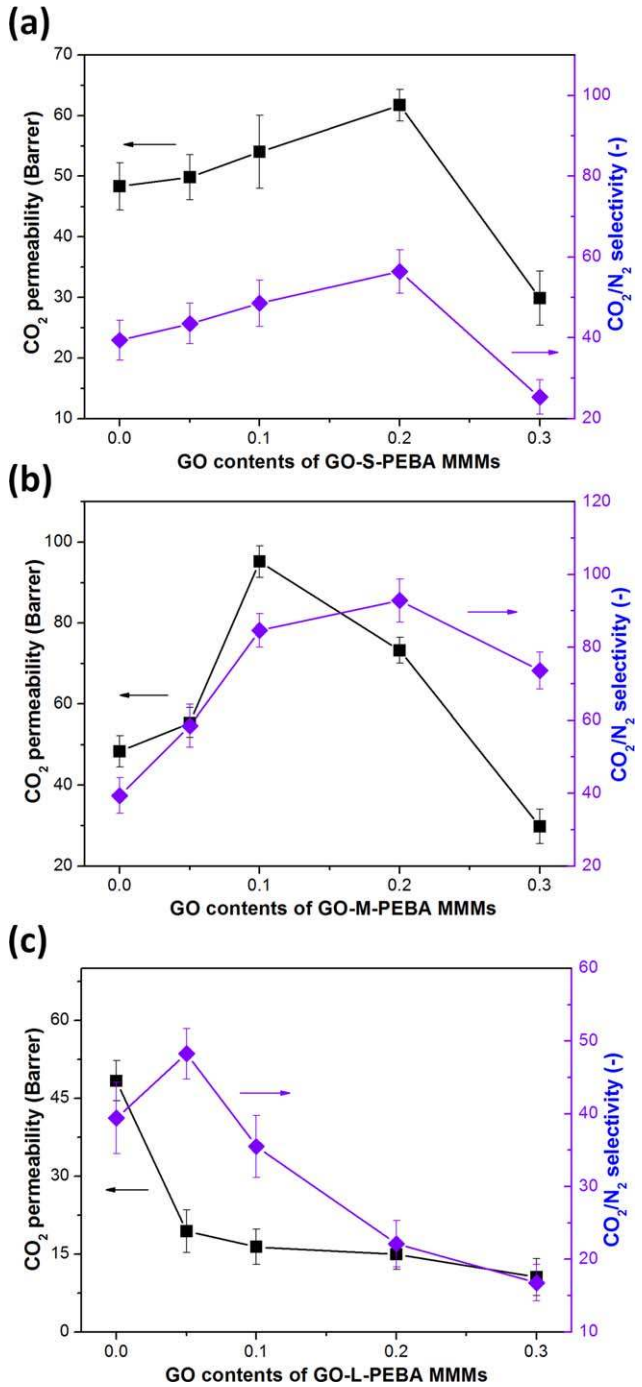

Figure 8. Effect of GO content on CO_2/N_2 separation performances (single gas separation) of (a) GO-S-PEBA, (b) GO-M-PEBA, and (c) GO-L-PEBA MMMs.

[Color figure can be viewed in the online issue, which is available at wileyonlinelibrary.com.]

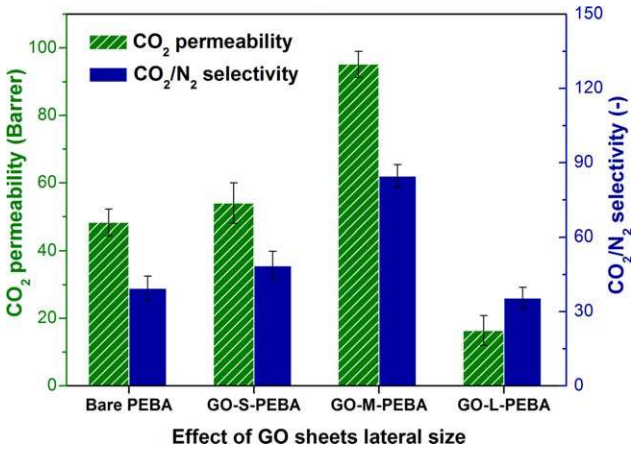

Figure 9. Effect of GO sheets lateral size on the CO_2/N_2 separation performance.

The GO contents were all 0.1 wt % in these membranes (single gas separation). [Color figure can be viewed in the online issue, which is available at wileyonlinelibrary.com.]

for the GO-S-PEBA membranes and 0.1 wt % for the GO-M-PEBA membranes. Before these "critical points," the membranes showed uniform dispersion of gas channels for efficient CO_2 transport, while after these "critical points," the gas permeability began to drop. As exhibited in Figures 8a, b, at high GO contents, the permeability and selectivity were both decreased, showing a poor dispersion of gas channels. Aggregation occurred when more GO was added, leading to a gas barrier effect. Meanwhile, GO sheets with larger lateral size were easier to show the gas barrier effect and poorer dispersion ability in polymeric environment. It is noted that the CO_2 permeability of the GO-S-PEBA membranes increased with the GO content from 0 to 0.2 wt % while for GO-M-PEBA membranes, the CO_2 permeability showed an obvious decrease at a GO content of 0.2 wt %. This can be ascribed to the larger GO sheets lateral size can lead to poor dispersion and easier formation of an aggregated stacking structure, which is detrimental to molecular transport. It was further proven by Figure 8c that the CO_2 permeability dropped continuously with GO content of sheets for the largest lateral size.

The potential energy barrier for gas permeation through the GO-based membrane is determined by many factors including membrane microstructure, physicochemical properties, and the GO lateral size. GO sheets can be engineered to well-defined laminates in polymeric environment and small sized gas molecules, especially CO_2, can diffuse between adjacent GO sheets. Therefore, GO sheets with appropriately large lateral size are beneficial for providing longer gas channels. As illustrated in Figure 9, compared with the bare PEBA membrane, the GO-S-PEBA membrane containing 0.1 wt % GO sheets with lateral sizes of 100–200 nm (Figure 1a) showed increased CO_2 permeability and CO_2/N_2 selectivity. This again proves that the GO laminates acted as gas channels for effective CO_2 permeation. When the GO lateral size was enlarged to 1–2 μm, the as-prepared membrane (with 0.1 wt % GO) exhibited the highest CO_2/N_2 separation performance among all the membranes. It has been proven that the larger GO sheets provided longer gas pathway, resulting in the fast-selective gas transport being further enhanced. Actually, XRD, DSC, and TGA all demonstrated that the mobility of the polymer molecules was tuned by the GO sheets lateral size, resulting in a strengthened restriction of polymer chains. As a result, the gas permeation was believed to be limited. However, the gas permeability increased dramatically when the GO sheets lateral size was in 1–2 μm. This further demonstrates the effect of the fast and selective gas channels built up by the GO sheets with suitable length. However, GO sheets with too large lateral size had a significantly negative influence on gas separation performance, as shown in Figure 9. CO_2 permeability was four times lower than that of the GO-M-PEBA membrane accompanied with a sharp decrease in CO_2/N_2 selectivity. This can be ascribed to the fact that the GO laminates generated with too large sized GO sheets tended to lie horizontally and were perpendicular to the molecular transport direction.[35] This can lead to a high energy barrier and severe hindrance of the gas permeation. As a result, GO lateral size is considered to effectively influence the molecular transport length, which is further explained in Supporting Information Figure 3.

Effect of operation parameters on CO_2/N_2 separation performance

Environmental conditions such as temperature and humidity can significantly influence the gas separation process. The effect

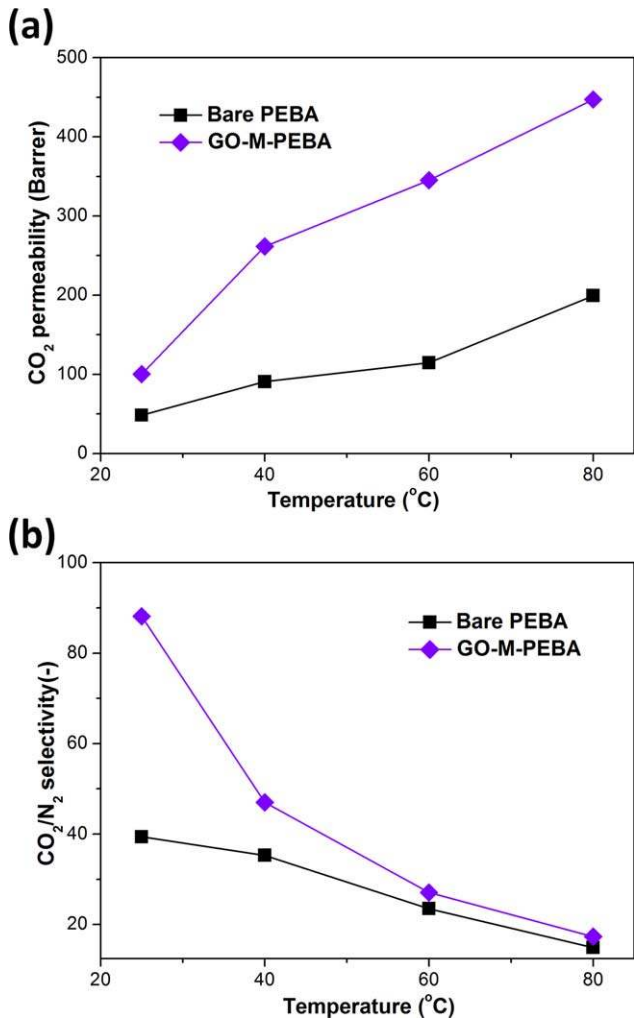

Figure 10. Effect of operation temperature on the CO_2/N_2 separation performance.

(a) and (b) are the CO_2 permeability and CO_2/N_2 selectivity, respectively (single gas separation). [Color figure can be viewed in the online issue, which is available at wileyonlinelibrary.com.]

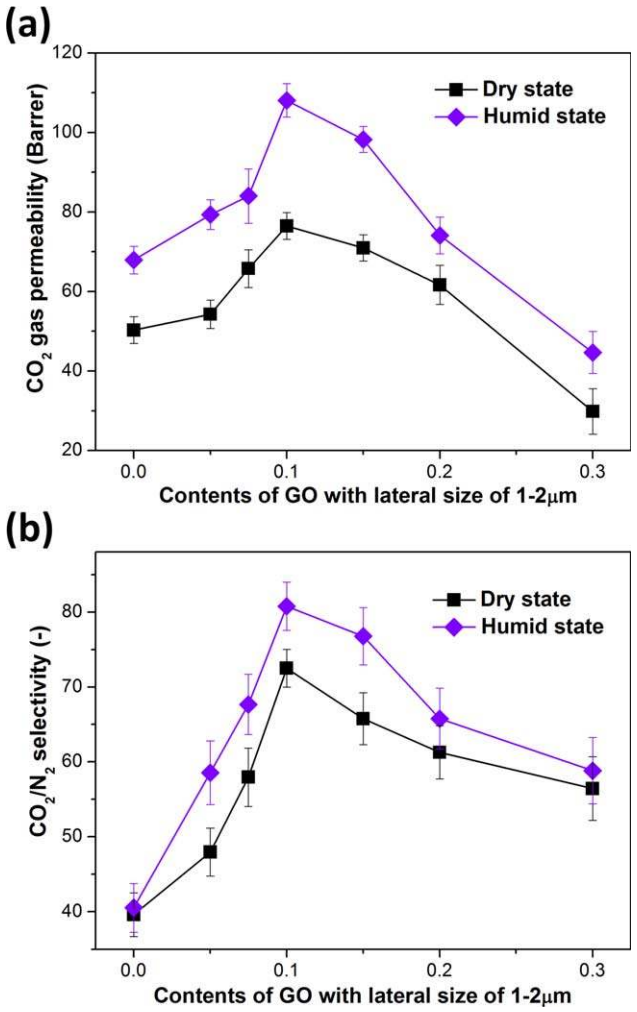

Figure 11. Effect of humidity on the mixed gas separation performance of CO_2/N_2 for GO-M-PEBA MMMs.

(a) and (b) are the CO_2 permeability and CO_2/N_2 selectivity, respectively (mixed gas separation). [Color figure can be viewed in the online issue, which is available at wileyonlinelibrary.com.]

of operation temperature on the gas permeation properties were first studied. The bare PEBA and GO-M-PEBA membranes are compared in Figure 10. Generally, membrane diffusivity is enhanced by temperature due to the increased flexibility of the polymer chains. With the increase of temperature, the CO_2 permeability for both membranes increased rapidly while the GO-M-PEBA membrane showed much faster CO_2 transport. This further demonstrates that the energy barrier for the GO-M-PEBA membrane is lower than for the bare PEBA membrane and that the GO laminates acted as fast and selective gas channels for efficient CO_2 separation. However, the CO_2/N_2 selectivity for both the bare PEBA and GO-M-PEBA membranes were decreased with temperature, even though the GO-M-PEBA membrane still showed higher selectivity than the bare PEBA membrane, for example, the CO_2/N_2 selectivity was 44% higher than that of the bare PEBA membrane at 40°C. This further proves that membranes with gas channels of GO laminates can realize selective CO_2 permeation, even at high temperatures.

The bare PEBA and GO-PEBA membranes were tested using a mixed gas of CO_2 and N_2 (50:50, vol %) in dry and humidified states, respectively (Figure 11). For the dry state permeation, it can be seen that the CO_2 permeability and CO_2/N_2 selectivity both increased with the incorporation of GO at low content, while they dropped at high GO content. These are in agreement with the results of the single gas permeation experiments. The selectivity slightly decreased on comparison with that of the single gas permeation tests, which is due to the competitive diffusion of the CO_2 and N_2 molecules. After humidifying, the CO_2 permeability for all membranes strongly increased due to the plasticization effect of the large amount of water molecules. Also, GO laminates in the membrane can adsorb water molecules[14] and thus the interlayer spacing can be enlarged, leading to an increase in gas permeability. No change was found for the CO_2/N_2 selectivity of the bare PEBA membrane after humidifying, which is in agreement with the literature.[53] For the GO-M-PEBA membranes, however, the CO_2/N_2 selectivity was apparently enhanced at relatively low GO content. This can be attributed to the large amount of uptake water molecules in the laminar GO transport channels, which can facilitate the hydration of CO_2 and the generation of HCO_3^-, which is beneficial for CO_2 molecules to permeate through the membrane with a lower energy barrier than N_2. When regards to high GO content, although the humidified CO_2 permeability was still higher than in the dry state, the selectivity was similar to that of dry membranes. This can be due to the aggregation at high GO content and the barrier effect beginning to dominate.

Long term operation testing

A long term continuous mixed gas permeation under humidified condition was carried out for more than 100 h, as shown in Figure 12. During the long term operation, the GO-M-PEBA membrane showed a high and stable separation performance under humidified condition, exhibiting a sturdy structure for practical implementation. This can be ascribed to the strong interaction between the GO sheets and polymer molecules. The CO_2 permeability held at about 110 Barrer with a high CO_2/N_2 selectivity of around 80. There were no defects formed during the long time testing in humidifying condition and the water-induced transport effect of the CO_2 molecules led to highly efficient CO_2 separation.

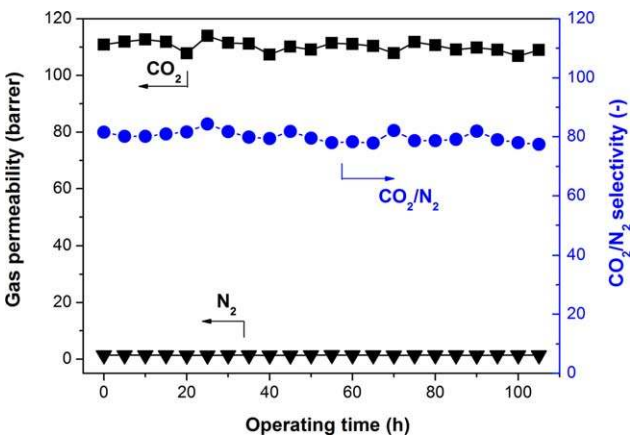

Figure 12. Long-term operation test of CO_2/N_2 mixed gas in humidified condition for GO-M-PEBA membrane with GO content of 0.1 wt % (mixed gas separation).

[Color figure can be viewed in the online issue, which is available at wileyonlinelibrary.com.]

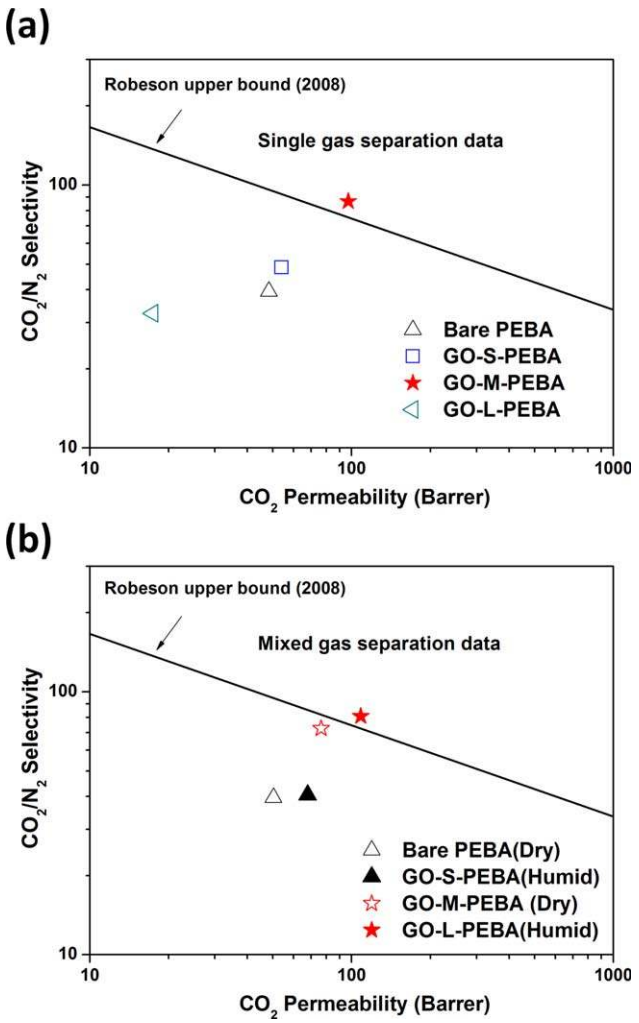

Figure 13. Comparison of CO_2/N_2 separation performances with Robeson upper-bound, (a) bare PEBA membrane and GO-PEBA MMMs (GO content: 0.1 wt %) with different lateral sizes (single gas separation data); (b) bare PEBA and GO-M-PEBA membrane (GO content: 0.1 wt %) in dry and humid states (mixed gas separation data).

[Color figure can be viewed in the online issue, which is available at wileyonlinelibrary.com.]

Comparison of CO_2/N_2 separation performance with upper-bound

As proven above, GO sheet lateral size is one of the most important factors for influencing the MMMs microstructures, physicochemical properties, and gas transport behaviors. It can tune polymer chains mobility and the polymer tended to be more rigid when the GO lateral size was increased. Even more importantly, the effective molecular transport length can be further manipulated by varying the GO lateral sizes. Figure 13a compares the CO_2/N_2 separation performances of the bare PEBA and GO-PEBA MMMs with different lateral sizes (GO content is 0.1 wt %). After incorporating GO sheets with lateral sizes of 100–200 nm and 1–2 μm, the GO-PEBA membranes showed an obvious increasing in the CO_2 separation performance, breaking the trade-off relationship. In particular, the GO-M-PEBA MMMs with 1–2 μm sized GO showed the highest CO_2 permeability as well as selectivity, transcending the 2008 upper-bound for polymeric membranes. This can be attributed to the fact that medium sized GO can be well-dispersed in polymer matrix and it showed a longer CO_2 transport length than that of GO sheets with lateral size of 100–200 nm. However, further increasing the lateral size to 5–10 μm led to a sharp decrease in separation performance. This is because the dispersibility was reduced when applying GO sheets too large in size. GO sheets with larger lateral sizes were believed to provide gas channels with longer transport lengths. However, they were inclined to lie in the horizontal direction due to the large aspect ratio. Thus, the GO laminates showed gas barrier effect rather than gas transporting property.

For the comparison of mixed gas separation, the performance of GO-M-PEBA is still much higher than that of bare PEBA, in spite of a slight decrease than the separation performance of single gas separation. As shown in Figure 13b, the developed GO-M-PEBA membrane showed an enhanced separation performance after humidifying, surpassing the CO_2/N_2 separation upper-bound, owing to the facilitate effect of water molecules in the GO-based membranes. It is thus beneficial for stably separating CO_2 from the real flue gas that contains water vapor. As a result, the as-prepared GO-PEBA MMMs manipulated by controlling the size effect of GO are promising for efficient CO_2 capture application.

Conclusion

In this work, GO sheets were engineered to fabricate the GO-PEBA MMMs and the effect of GO lateral size was investigated in detail. It can be found that the lateral size of GO sheets can significantly influence the membrane microstructure and physicochemical properties. The mobility of polymer chains was restricted with increasing GO lateral size. Moreover, large sized GO can cause poor dispersion properties in membranes, leading to the gas barrier effect. The effects of different operation conditions, such as temperature and humidity, on the membrane separation performances were also investigated. After systematic optimization, the GO-PEBA membrane containing 0.1 wt % GO sheets with lateral sizes of 1–2 μm was obtained, exhibiting excellent and stable CO_2/N_2 separation performance with CO_2 permeability of 110 Barrer and CO_2/N_2 selectivity of 80. The optimized GO-PEBA MMMs with fast and selective gas channels are promising for practical application for CO_2 capture.

Acknowledgments

This work was financially supported by the National Natural Science Foundation of China (Grant Nos. 21476107, 21490585, 21406107), the Innovative Research Team Program by the Ministry of Education of China (Grant No. IRT13070), a Project funded by the Priority Academic Program Development of Jiangsu Higher Education Institutions (PAPD), the Innovation Project of Graduate Research by Jiangsu Province (Grant No. KYLX_0764) and Top-notch Academic Programs Project of Jiangsu Higher Education Institutions (TAPP).

Literature Cited

1. Koros WJ, Fleming GK. Membrane-based gas separation. *J Membr Sci*. 1993;83:1–80.
2. Bernal MP, Coronas J, Menéndez M, Santamaría J. Separation of CO2/N2 mixtures using MFI-type zeolite membranes. *AIChE J*. 2004;50:127–135.
3. Poshusta JC, Tuan VA, Pape EA, Noble RD, Falconer JL. Separation of light gas mixtures using SAPO-34 membranes. *AIChE J*. 2000;46: 779 –789.

4. Robeson LM. Correlation of separation factor versus permeability for polymeric membranes. *J Membr Sci*. 1991;62:165–185.
5. Moore TT, Mahajan R, Vu DQ, Koros WJ. Hybrid membrane materials comprising organic polymers with rigid dispersed phases. *AIChE J*. 2004;50:311–321.
6. Hao L, Zuo J, Chung T-S. Formation of defect-free polyetherimide/PIM-1 hollow fiber membranes for gas separation. *AIChE J*. 2014; 60:3848–3858.
7. Novoselov KS, Geim AK, Morozov SV, Jiang D, Zhang Y, Dubonos SV, Grigorieva IV, Firsov AA. Electric field effect in atomically thin carbon films. *Science*. 2004;306:666–669.
8. Geim AK, Novoselov KS. The rise of graphene. *Nat Mater*. 2007;6: 183–191.
9. Nair RR, Wu HA, Jayaram PN, Grigorieva IV, Geim AK. Unimpeded permeation of water through helium-leak–tight graphene-based membranes. *Science*. 2012;335:442–444.
10. Liu G, Jin W, Xu N. Graphene-based membranes. *Chem Soc Rev*. 2015;44:5016–5030.
11. Perreault F, Fonseca de Faria A, Elimelech M. Environmental applications of graphene-based nanomaterials. *Chem Soc Rev*. 2015;44:5861–5896.
12. Cohen-Tanugi D, Grossman JC. Water desalination across nanoporous graphene. *Nano Lett*. 2012;12:3602–3608.
13. Lou Y, Liu G, Liu S, Shen J, Jin W. A facile way to prepare ceramic-supported graphene oxide composite membrane via silane-graft modification. *Appl Surf Sci*. 2014;307:631–637.
14. Huang K, Liu G, Lou Y, Dong Z, Shen J, Jin W. A graphene oxide membrane with highly selective molecular separation of aqueous organic solution. *Angew Chem Int Ed*. 2014;53:6929–6932.
15. Huang K, Liu G, Shen J, Chu Z, Zhou H, Gu X, Jin W, Xu N. High-efficiency water-transport channels using the synergistic effect of a hydrophilic polymer and graphene oxide laminates. *Adv Funct Mater*. 2015;25:5809–5815.
16. Kim HW, Yoon HW, Yoon S-M, Yoo BM, Ahn BK, Cho YH, Shin HJ, Yang H, Paik U, Kwon S, Choi J-Y, Park HB. Selective gas transport through few-layered graphene and graphene oxide membranes. *Science*. 2013;342:91–95.
17. Smith ZP, Freeman BD. Graphene oxide: a new platform for high-performance gas- and liquid-separation membranes. *Angew Chem Int Ed*. 2014;53:10286–10288.
18. Zhu J, Chen M, He Q, Shao L, Wei S, Guo Z. An overview of the engineered graphene nanostructures and nanocomposites. *RSC Adv*. 2013;3:22790–22824.
19. Paulus GLC, Shimizu S, Abrahamson JT, Zhang J, Hilmer AJ, Strano MS. The chemical engineering of low-dimensional materials. *AIChE J*. 2011;57:1104–1118.
20. Vu DQ, Koros WJ, Miller SJ. Mixed matrix membranes using carbon molecular sieves: I. Preparation and experimental results. *J Membr Sci*. 2003;211:311–334.
21. Vu DQ, Koros WJ, Miller SJ. Mixed matrix membranes using carbon molecular sieves: II. Modeling permeation behavior. *J Membr Sci*. 2003;211:335–348.
22. Ahn J, Chung W-J, Pinnau I, Guiver MD. Polysulfone/silica nanoparticle mixed-matrix membranes for gas separation. *J Membr Sci*. 2008;314:123–133.
23. Liu G, Hung W-S, Shen J, Li Q, Huang Y-H, Jin W, Lee K-R, Lai J-Y. Mixed matrix membranes with molecular-interaction-driven tunable free volumes for efficient bio-fuel recovery. *J Mater Chem A*. 2015;3:4510–4521.
24. Zornoza B, Téllez C, Coronas J, Esekhile O, Koros WJ. Mixed matrix membranes based on 6FDA polyimide with silica and zeolite microsphere dispersed phases. *AIChE J*. 2015;61:4481–4490.
25. Süer MG, Baç N, Yilmaz L. Gas permeation characteristics of polymer-zeolite mixed matrix membranes. *J Membr Sci*. 1994;91:77–86.
26. Snyder MA, Tsapatsis M. Hierarchical nanomanufacturing: from shaped zeolite nanoparticles to high-performance separation membranes. *Angew Chem Int Ed*. 2007;46:7560–7573.
27. Liu G, Xiangli F, Wei W, Liu S, Jin W. Improved performance of PDMS/ceramic composite pervaporation membranes by ZSM-5 homogeneously dispersed in PDMS via a surface graft/coating approach. *Chem Eng J*. 2011;174:495–503.
28. Kim S, Marand E, Ida J, Guliants VV. Polysulfone and mesoporous molecular sieve MCM-48 mixed matrix membranes for gas separation. *Chem Mater*. 2006;18:1149–1155.
29. Li D, Wang H. Recent developments in reverse osmosis desalination membranes. *J Mater Chem*. 2010;20:4551–4566.
30. Liu S, Liu G, Zhao X, Jin W. Hydrophobic-ZIF-71 filled PEBA mixed matrix membranes for recovery of biobutanol via pervaporation. *J Membr Sci*. 2013;446:181–188.
31. Liu S, Liu G, Shen J, Jin W. Fabrication of MOFs/PEBA mixed matrix membranes and their application in bio-butanol production. *Sep Purif Technol*. 2014;133:40–47.
32. Ganesh BM, Isloor AM, Ismail AF. Enhanced hydrophilicity and salt rejection study of graphene oxide-polysulfone mixed matrix membrane. *Desalination*. 2013;313:199–207.
33. Zinadini S, Zinatizadeh AA, Rahimi M, Vatanpour V, Zangeneh H. Preparation of a novel antifouling mixed matrix PES membrane by embedding graphene oxide nanoplates. *J Membr Sci*. 2014;453:292–301.
34. Li H, Song Z, Zhang X, Huang Y, Li S, Mao Y, Ploeh HJ, Bao Y, Yu M. Ultrathin, molecular-sieving graphene oxide membranes for selective hydrogen separation. *Science*. 2013;342:95–98.
35. Shen J, Liu G, Huang K, Jin W, Lee K-R, Xu N. Membranes with fast and selective gas-transport channels of laminar graphene oxide for efficient CO_2 capture. *Angew Chem Int Ed*. 2015;54:578–582.
36. Su Y, Kravets V, Wong S, Waters J, Geim A, Nair R. Impermeable barrier films and protective coatings based on reduced graphene oxide. *Nat commun*. 2014;5.
37. Yang YH, Bolling L, Priolo MA, Grunlan JC. Super gas barrier and selectivity of graphene oxide-polymer multilayer thin films. *Adv Mater*. 2013;25:503–508.
38. Chen J-T, Fu Y-J, An Q-F, Lo SC, Huang S-H, Hung W-S, Hu C-C, Lee K-R, Lai J-Y. Tuning nanostructure of graphene oxide/polyelectrolyte LbL assemblies by controlling pH of GO suspension to fabricate transparent and super gas barrier films. *Nanoscale* 2013;5:9081–9088.
39. Sun P, Zheng F, Zhu M, Song Z, Wang k, Zhong M, Wu D, Litte RB, Xu Z, Zhu H. Selective Trans-membrane transport of alkali and alkaline earth cations through graphene oxide membranes based on cation$-\pi$ Interactions. *ACS Nano*. 2014;8:850–859.
40. Chung T-S, Jiang LY, Li Y, Kulprathipanja S. Mixed matrix membranes (MMMs) comprising organic polymers with dispersed inorganic fillers for gas separation. *Prog Polym Sci*. 2007;32:483–507.
41. Wee LH, Li Y, Zhang K, Davit P, Bordiga S, Jiang J, Vankelecom IFJ, Martens JA. Submicrometer-sized ZIF-71 filled organophilic membranes for improved bioethanol recovery: mechanistic insights by Monte Carlo simulation and FTIR spectroscopy. *Adv Funct Mater*. 2015;25:516–525.
42. Hummers WS, Offeman RE. Preparation of graphitic oxide. *J Am Chem Soc*. 1958;80:1339–1339.
43. Huang K, Dong Z, Li Q, Jin W. Growth of a ZIF-8 membrane on the inner-surface of a ceramic hollow fiber via cycling precursors. *Chem Commun*. 2013;49:10326–10328.
44. Li D, Kaner RB. Graphene-based materials. *Science*. 2008;320: 1170–1171.
45. Dreyer DR, Park S, Bielawski CW, Ruoff RS. The chemistry of graphene oxide. *Chem Soc Rev*. 2010;39:228–240.
46. Ferrari AC, Robertson J. Interpretation of Raman spectra of disordered and amorphous carbon. *Phys Rev B*. 2000;61:14095–14107.
47. Graf D, Molitor F, Ensslin K, Stampfer C, Jungen A, Hierold C, Wirtz L. Spatially resolved raman spectroscopy of single- and few-layer graphene. *Nano Lett*. 2007;7:238–242.
48. Car A, Stropnik C, Yave W, Peinemann K-V. PEG modified poly(-amide-b-ethylene oxide) membranes for CO_2 separation. *J Membr Sci*. 2008;307:88–95.
49. Dikin DA, Stankovich S, Zimney EJ, Piner RD, Dommett GHB, Evmenenko G, Nguyen ST, Ruoff RS. Preparation and characterization of graphene oxide paper. *Nature* 2007;448:457–460.
50. Kim JH, Lee YM. Gas permeation properties of poly(amide-6-b-ethylene oxide)–silica hybrid membranes. *J Membr Sci*. 2001;193: 209–225.
51. Bondar VI, Freeman BD, Pinnau I. Gas sorption and characterization of poly(ether-b-amide) segmented block copolymers. *J Polym Sci Polym Phys*. 1999;37:2463–2475.
52. Sridhar S, Suryamurali R, Smitha B, Aminabhavi TM. Development of crosslinked poly(ether-block-amide) membrane for CO_2/CH_4 separation. *Colloid Surf A*. 2007;297:267–274.
53. Li Y, Xin Q, Wu H, Guo R, Tian Z, Liu Y, Wang S, He G, Pan F, Jiang Z. Efficient CO_2 capture by humidified polymer electrolyte membranes with tunable water state. *Energy Environ Sci*. 2014;7:1489–1499.

Manuscript received Nov. 24, 2015, and revision received Mar. 8, 2016.